Accounting for Stream–Aquifer Interactions in the State-Space Discretization of the Kalinin–Milyukov–Nash Cascade for Streamflow Forecasting

Jozsef Szilagyi[1]

Abstract: A sample-data system discretization of the continuous Kalinin–Milyukov–Nash cascade is performed in a state-space analysis framework allowing for stream–aquifer interactions that include bank storage during flood events and groundwater discharge to the stream under low-flow conditions. These interactions generally result in faster attenuation of propagating flood waves and in elevated streamflow levels during drought conditions. An example is given that demonstrates how accounting for these processes ensures more reliable streamflow forecasts. The model is based on a simplified physical description of the processes both in the stream and across the stream–aquifer boundary.

DOI: 10.1061/(ASCE)1084-0699(2004)9:2(135)

CE Database subject headings: Base flow; Flood routing; Streamflow forecasting; Wave attenuation.

Introduction

The floods of 2002 wreaked havoc all over Central Europe, causing mass evacuations, numerous deaths and extensive damage with costs in the billions of euros (Pearce 2002). The floods were triggered by precipitation of unusually high intensity and/or of duration. For example, the Czech Republic experienced four times its normal precipitation for August in just 36 h (Pearce 2002). Although not yet proven, the floods may have been exacerbated by global warming, resulting in elevated levels of meltwater from Alpine glaciers (Pearce 2002). If one considers that 10% of Europe's population lives or works on flood plains (in Hungary, 25% of a population of 10 million) and that the Danube, the continent's second largest river after the Volga, had two 100-year floods in the past 11 years (Pearce 2002), then one realizes the importance and value of accurate and reliable flood forecasts in the region.

The National Hydrological Forecasting Service (NHFS) in Hungary prepares streamflow forecasts for the Danube and its tributaries every day with 1–3 days of leadtime. The reliability of these estimates undoubtedly played a role in ensuring that Hungary did not suffer bigger losses in property during the Danube's record-breaking flood of the summer of 2002. By knowing in advance when, where, and at what level the river would crest, flood protection works could be planned and organized. The NHFS uses a state-space formulated discretized version of the continuous Kalinin–Milyukov–Nash (KMN) cascade for streamflow routing. However, the model, called the discrete linear cascade model (DLCM), does not explicitly account for stream–aquifer interactions, and that lack catalyzed the present work: to formulate a version of the state-space framework that would make it possible to include such interactions in future versions of the model.

[1]Research Hydrologist/Associate Professor, Conservation and Survey Division, Univ. of Nebraska-Lincoln, Lincoln, NE 68588-0517. E-mail: jszilagyi1@unl.edu

Note. Discussion open until August 1, 2004. Separate discussions must be submitted for individual papers. To extend the closing date by one month, a written request must be filed with the ASCE Managing Editor. The manuscript for this paper was submitted for review and possible publication on October 18, 2002; approved on July 22, 2003. This paper is part of the ***Journal of Hydrologic Engineering***, Vol. 9, No. 2, March 1, 2004. ©ASCE, ISSN 1084-0699/2004/2-135–143/$18.00.

Sample-Data System Description of Discrete Linear Cascade Model for Streamflow Forecasting

The DLCM is a discretized version of a cascade of linear reservoirs with inputs and outputs continuous in time. Nash (1957), and independently of him, Kalinin and Milyukov (1957), used such a cascade for rainfall runoff and flow routing problems, respectively. The linear cascade model is often called the Nash cascade, but perhaps it is more correct to call it the KMN cascade (Szöllősi-Nagy 1989) in a tribute to the other two hydrologists who first applied it to flow routing as is explored here. Cunge (1969) pointed out the tight relationship of the KMN cascade to the linear kinematic wave equation, the latter being a first-order approximation of the Saint–Venant equations that describe the flow in open channels. The linear kinematic wave equation can be written as

$$\frac{\partial Q(x,t)}{\partial t} + C\frac{\partial Q(x,t)}{\partial x} = 0 \tag{1}$$

where Q = flowrate $[\mathrm{L}^3\,\mathrm{T}^{-1}]$; C = kinematic wave celerity $[\mathrm{L}\,\mathrm{T}^{-1}]$; and x and t = spatial and temporal coordinates, respectively. Using a backward-difference scheme in the spatial derivatives, Eq. (1) can be written as

$$\frac{\partial Q(x_j,t)}{\partial t} = -C\frac{Q(x_j,t)-Q(x_{j-1},t)}{\Delta x}$$

$$= \frac{C}{\Delta x}Q(x_{j-1},t) - \frac{C}{\Delta x}Q(x_j,t) \tag{2}$$

with $x_j = j\Delta x$; and $j = 1,2,\ldots,n$. Eq. (2) may represent a given stream reach with no lateral inflow, divided into n sections.

For the state-space formulation of Eq. (2), one can define the state variable as $\mathbf{Q}(t)=[Q(x_{1,t}),Q(x_{2,t}),\ldots,Q(x_{n,t})]'=[Q_1(t),Q_2(t),\ldots,Q_n(t)]'$ where the prime denotes the transpose of the vector. By denoting the inflow to the reach as $u(t)=Q(x_0,t)$ one can write Eq. (2) as

$$\begin{bmatrix} \frac{dQ_1(t)}{dt} \\ \frac{dQ_2(t)}{dt} \\ \vdots \\ \frac{dQ_n(t)}{dt} \end{bmatrix} = \begin{bmatrix} -\frac{C}{\Delta x} & 0 & \cdots & 0 \\ \frac{C}{\Delta x} & -\frac{C}{\Delta x} & \ddots & \vdots \\ & \ddots & \ddots & 0 \\ 0 & & \frac{C}{\Delta x} & -\frac{C}{\Delta x} \end{bmatrix} \begin{bmatrix} Q_1(t) \\ Q_2(t) \\ \vdots \\ Q_n(t) \end{bmatrix} + \begin{bmatrix} \frac{C}{\Delta x} \\ 0 \\ \vdots \\ 0 \end{bmatrix} u(t) \tag{3}$$

which in a more succinct form becomes

$$\dot{\mathbf{Q}}(t)=\underline{\underline{F}}\mathbf{Q}(t)+\mathbf{G}u(t) \tag{4a}$$

where the dot denotes the temporal change in the state-variable $\mathbf{Q}$. Eq. (4*a*) is the state equation of a linear, continuous dynamic system with time-invariant coefficient matrices. Here $\underline{\underline{F}}$ is the system matrix and $\mathbf{G}$ the distribution vector (Szöllősi-Nagy 1989). The output equation of the system can be written as

$$Q_{\text{out}}(t)=\mathbf{H}\mathbf{Q}(t) \tag{4b}$$

with $\mathbf{H}$ in our example defined as $\mathbf{H}=[0,0,\ldots,1]$, a $1\times n$ vector, so that Eq. (4*b*) provides a scalar output: $Q_{\text{out}}(t)=Q(x_n,t)$.

For a linear reservoir, the outflow is linearly related to the stored water, $Q(t)=kS(t)$, where k^{-1} (T) is the storage coefficient. Assuming that each subreach behaves as a linear reservoir with $C/\Delta x=k$, Eq. (3) transforms into

$$\begin{bmatrix} \frac{dS_1(t)}{dt} \\ \frac{dS_2(t)}{dt} \\ \vdots \\ \frac{dS_n(t)}{dt} \end{bmatrix} = \begin{bmatrix} -k & 0 & \cdots & 0 \\ k & -k & \ddots & \vdots \\ & \ddots & \ddots & 0 \\ 0 & & k & -k \end{bmatrix} \begin{bmatrix} S_1(t) \\ S_2(t) \\ \vdots \\ S_n(t) \end{bmatrix} + \begin{bmatrix} 1 \\ 0 \\ \vdots \\ 0 \end{bmatrix} u(t) \tag{5}$$

with $\mathbf{H}=[0,0,\ldots,k]$ in $Q_{\text{out}}(t)=\mathbf{H}\mathbf{S}(t)$. Eq. (5) is the state-space representation of the continuous KMN cascade (Szöllősi-Nagy 1989).

Due to the fact that streamflow measurements become discrete values on the digital computer, a discretization of Eq. (5) must be performed to have a streamflow model compatible with the discrete nature of its inputs. Szöllősi-Nagy (1982) performed the discretization of Eq. (5) using a pulse-data system, while Szilagyi (2003) did the same for a sample-data system and showed that this latter approach is a generalization of the former, meaning that if the discretization is done with the sample-data system then, without changing the model structure, one can simply use it with pulsed data as well, typically with precipitation data, most often available in a pulsed format. A sample-data system assumes that the input variable changes linearly between successive discrete data values, while the pulse-data system assumes a constant value (e.g., Chow et al. 1988). Szilagyi (2003) demonstrates the steps involved with the derivation of discretizing Eq. (5) in a sample-data system. Here we show only the result of the discretization through which Eq. (5) transforms into

$$\mathbf{S}(t+\Delta t)=\underline{\underline{\Phi}}(\Delta t)\mathbf{S}(t)+\mathbf{\Gamma}_1(\Delta t)u(t+\Delta t)-\mathbf{\Gamma}_2(\Delta t)u(t) \tag{6}$$

where $\underline{\underline{\Phi}}$=state-transition matrix; and $\mathbf{\Gamma}_1$ and $\mathbf{\Gamma}_2$=input-transition vectors. The $n\times n$ matrix of $\underline{\underline{\Phi}}$ is made up of the following terms:

$$\underline{\underline{\Phi}}(\Delta t)=\begin{bmatrix} e^{-k\Delta t} & 0 & \cdots & 0 \\ k\Delta t e^{-k\Delta t} & e^{-k\Delta t} & \ddots & \vdots \\ \vdots & \vdots & \ddots & 0 \\ \frac{(k\Delta t)^{n-1}}{(n-1)!}e^{-k\Delta t} & \frac{(k\Delta t)^{n-2}}{(n-2)!}e^{-k\Delta t} & \cdots & e^{-k\Delta t} \end{bmatrix} \tag{7}$$

while $\mathbf{\Gamma}_1$ and $\mathbf{\Gamma}_2$ are

$$\mathbf{\Gamma}_1(\Delta t)=\begin{bmatrix} \frac{1}{k}\frac{\Gamma(1,k\Delta t)}{\Gamma(1)}\left[1+\frac{e^{-k\Delta t}}{\Gamma(1,k\Delta t)}-\frac{1}{k\Delta t}\right] \\ \frac{1}{k}\frac{\Gamma(2,k\Delta t)}{\Gamma(2)}\left[1+\frac{k\Delta t e^{-k\Delta t}}{\Gamma(2,k\Delta t)}-\frac{2}{k\Delta t}\right] \\ \vdots \\ \frac{1}{k}\frac{\Gamma(n,k\Delta t)}{\Gamma(n)}\left[1+\frac{(k\Delta t)^{n-1}e^{-k\Delta t}}{\Gamma(n,k\Delta t)}-\frac{n}{k\Delta t}\right] \end{bmatrix} \tag{8}$$

and

$$\mathbf{\Gamma}_2(\Delta t)=\begin{bmatrix} \frac{1}{k}\frac{\Gamma(1,k\Delta t)}{\Gamma(1)}\left[\frac{e^{-k\Delta t}}{\Gamma(1,k\Delta t)}-\frac{1}{k\Delta t}\right] \\ \frac{1}{k}\frac{\Gamma(2,k\Delta t)}{\Gamma(2)}\left[\frac{k\Delta t e^{-k\Delta t}}{\Gamma(2,k\Delta t)}-\frac{2}{k\Delta t}\right] \\ \vdots \\ \frac{1}{k}\frac{\Gamma(n,k\Delta t)}{\Gamma(n)}\left[\frac{(k\Delta t)^{n-1}e^{-k\Delta t}}{\Gamma(n,k\Delta t)}-\frac{n}{k\Delta t}\right] \end{bmatrix} \tag{9}$$

respectively. The function, denoted by Γ within $\mathbf{\Gamma}_1$ and $\mathbf{\Gamma}_2$, is the incomplete (with two arguments, i.e., $\Gamma(a,\xi)=\int_0^\xi e^{-t}t^{a-1}dt$), or complete (with one argument, i.e., $\Gamma(a)=\int_0^\infty e^{-t}t^{a-1}dt$), gamma function, respectively. All system matrices are time invariant and only depend on the magnitude of the sampling interval Δt. Note that time now increases with an increment of Δt. Using a recursion in Eq. (6), the output at $t=m\Delta t$ becomes

$$Q_{\text{out}}(m\Delta t)=\mathbf{H}\mathbf{S}(m\Delta t)=\mathbf{H}\underline{\underline{\Phi}}^m(\Delta t)\mathbf{S}(0)+\sum_{i=0}^{m-1}\mathbf{H}\underline{\underline{\Phi}}^{m-1-i}(\Delta t)\times[\mathbf{\Gamma}_1(\Delta t)u[(i+1)\Delta t]-\mathbf{\Gamma}_2(\Delta t)u(i\Delta t)] \tag{10}$$

Eq. (10) also shows how storage ($\mathbf{S}$) changes in time with discrete time increments (once the initial condition is defined at $t=0$) in response to discrete inputs and assuming a linear change in the input variable between its discrete values. Here $\underline{\underline{\Phi}}^m(\Delta t)=\underline{\underline{\Phi}}(m\Delta t)$ (Szöllősi-Nagy 1982).

The advantage of using a state-space approach over a numerical solution of Eq. (1) is at least fourfold: (1) the numerical solution of Eq. (1) with a given Δt will depend on four parameters: the temporal and spatial increments used during the integration that will influence the magnitude of the numerical diffusion (Cunge 1969); the error limit of convergence; and the celerity parameter (C), which needs to be optimized for a given input–

output discrete time series. In the state-space approach, the solution [Eq. (10)] requires only algebraic manipulations which do not involve any convergence of trial values, and it depends on only two parameters, n and k, to be optimized for a given input–output sequence; (2) in the state-space approach, once a solution is obtained for a given Δt, any new solution with a different Δt can be obtained from the first result by a linear transformation without the need of redoing the original calculations (Szöllősi-Nagy 1982), unlike in the case of numerical solutions; (3) when minimizing model error, an important task in operational forecasting, one can use an optimal filter (Kalman 1960; Kalman and Bucy 1961) in a straightforward manner provided the model is in a state-space form; (4) the inverse problem in forecasting, the so-called input detection (i.e., finding the input sequence to a given output sequence), which often is needed to fill gaps of missing data in streamflow series, is again a simple algebraic manipulation with the state-space framework (Szöllősi-Nagy 1982).

Formulation of Simplified Stream–Aquifer Interactions

As the floodwave travels in the stream, part of its volume is being stored in the streambank due to a reversed hydraulic gradient between groundwater and streamwater. This causes a flattening of the propagating floodwave in addition to diffusional effects. The stored water in the banks may later be released, together with baseflow, into the stream, when the hydraulic gradient changes back to its normal position for groundwater-fed streams. In catchments where infiltration rates are high, such as the Sandhills region of Nebraska, a significant portion of the streamflow [as high as 90% (Szilagyi et al. 2003)] may be maintained year round by such groundwater discharge (i.e., baseflow) to the stream. However, not all the water stored in the streambank may find its way back to the stream, because varying parts of it may be taken up by vegetation and released to the air via transpiration.

Accounting for this dynamic interaction between stream and aquifer, though it be simplistic, will improve streamflow forecasts. Here the objective is to find a description that fits into the existing structure of the state-space model when allowing for stream–aquifer interactions, and to do it with a minimal number of additional parameters. Parameter parsimony is an important requirement of operative forecasting models, especially when the parameters must be optimized and from time to time need updating for a large number of gaging stations. For example, the state-space forecasting model of the Danube and its tributaries in Hungary contains 50 plus gaging stations. If only four parameters need to be optimized and updated for each station in the model, it immediately means 200 plus parameters. The problem is further complicated by the common practice that only stream levels are monitored, while groundwater elevations adjacent to gaging stations are not, nor is information typically available on the geometry and hydraulic properties of the aquifer. This complicates the validation of any model that describes stream–aquifer interactions. The only venue to pursue, and also the most important one for the purpose of streamflow forecasting, is to check if the employed model, however simplistic, improves forecasts or not. These conditions must be kept in mind when judging the below derived description of stream–aquifer interactions to be included in the state-space model of constant coefficient matrices.

Contribution of stream-aquifer interactions to flood routing is well established (e.g. Pinder and Sauer 1971; Zitta and Wiggert 1971; Moench et al. 1974; Hunt 1990; Hantush et al. 2001, 2002). Here we follow the problem description of Hantush et al. (2002) by writing out the linearized version of the Boussinesq equation

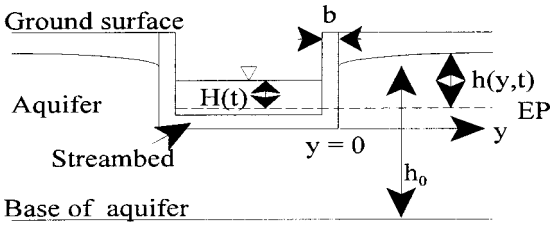

Fig. 1. Schematics of stream–aquifer system

$$\frac{\partial h(y,t)}{\partial t} = D\frac{\partial^2 h(y,t)}{\partial y^2} \tag{11}$$

with initial and boundary conditions

$$h(y,0) = 0 \tag{12}$$

$$q(t) = -T\frac{\partial h(0,t)}{\partial y} = PK'\frac{H(t)-h(0,t)}{b} \tag{13}$$

$$h(\infty,t) = 0 \tag{14}$$

where $h(y,t)$ [L] denotes the groundwater-table elevation relative to its initial equilibrium position when the groundwater table is assumed to be horizontal and at the same elevation with the streamstage. D [$L^2 T^{-1}$] = aquifer diffusivity; $D = TS_y^{-1} = Kh_0 S_y^{-1}$, where T [$L^2 T^{-1}$] = its average transmissivity, K [$L T^{-1}$] is saturated hydraulic conductivity; h_0 [L] = average saturated thickness; and S_y (-) is the specific yield of the unconfined aquifer. $H(t)$ [L] = streamstage relative to its initial equilibrium position; P [L] = one half of the average wetted perimeter of the stream; K' [$L T^{-1}$] = mean saturated hydraulic conductivity of the streambed with an average thickness of b [L]; and $q(t)$ [$L^2 T^{-1}$] = resulting flowrate between the stream and the aquifer over a unit length. See Fig. 1 for a schematic of the situation.

The following assumptions were made in formulating the problem (Hantush et al. 2002): (1) the aquifer is homogeneous with a horizontal bed; (2) groundwater-table fluctuations are small compared to the average saturated thickness (h_0) of the aquifer; (3) storage in aquifer sediments below the stream is negligible; (4) water-level fluctuations along the stream reach are small compared to the average stage $H(t)$.

Eqs. (11)–(14) can be coupled to streamflow through the following continuity equation for each subreach of the stream:

$$\frac{dS_j(t)}{dt} = Q(x_{j-1},t) - Q(x_j,t) - 2q_L(t) \tag{15}$$

where it was considered that the stream has two banks and that $q_L(t)$ [$L^3 T^{-1}$], which is $q(t)$ integrated over the length of the subreach, changes signs between Eqs. (13) and (15), because a loss of water to the aquifer is a gain to the stream.

As can be seen from Eqs. (11) and (13), $q_L(t)$ depends on the combination of two parameters: D and $\gamma (= PK'b^{-1})$. The objective here is not an accurate description of the elevation of the groundwater table through time [$h(y,t)$], but simply the estimation of $q_L(t)$ in terms of stream storage (if possible), so that the state equation [Eq. (5)] could be augmented by this term. As a consequence, a combination of the D and γ parameter values is sought that is suitable for the estimation of $q_L(t)$, without much

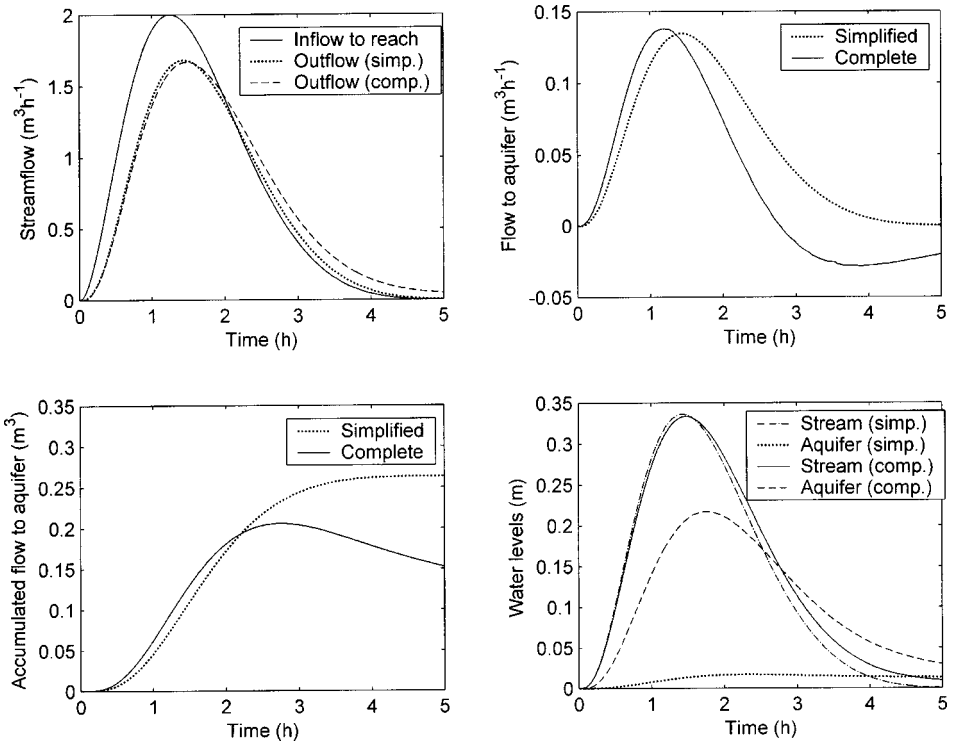

Fig. 2. Numerical solution of Eqs. (11)–(15) with complete and simplified boundary conditions: (a) in- and outflow from the reach; (b) flux across stream–aquifer interface; (c) accumulated flux across stream–aquifer interface; (d) water levels in stream and in aquifer, $h(0,t)$, adjacent to stream. With complete boundary condition $\gamma=1\ \mathrm{m\,h^{-1}}$, $D=0.5\ \mathrm{m^2\,h^{-1}}$, and $\gamma=0.4\ \mathrm{m\,h^{-1}}$, $D=100\ \mathrm{m^2\,h^{-1}}$ with simplified boundary condition

concern for how accurate the corresponding $h(y,t)$ values are. In fact, we will postulate that the diffusivity of the aquifer is considered large enough for our purposes that any water that crosses the streambed from the stream is distributed so quickly in the semi-infinite aquifer that the change in $h(0,t)$ can be considered negligible and so it becomes a constant c_h.

To illustrate that such a deliberate combination of the D and γ parameter values is meaningful, Eqs. (11)–(15) were numerically solved in a coupled stream–aquifer finite-elements model with inflow $I(t)$ to the stream reach (having a rectangular cross section of unit length and width, coupled to a 10 m wide aquifer) defined as (Hantush et al. 2002)

$$I(t)=NI_{\max}e^{-\delta t}[1-\cos(\omega t)] \quad 0\leqslant t\leqslant \Delta T \tag{16a}$$

$$I(t)=0 \quad t>\Delta T \tag{16b}$$

where $I_{\max}=2\ \mathrm{m^3\,h^{-1}}=$peak inflow rate; $\Delta T=5$ h=duration of the floodwave; $\omega=2\pi/\Delta T$, $N=e^{\delta t_c}[1-\cos(\omega t_c)]^{-1}$ with $t_c=1.25$ h, the time when peak inflow occurs; and $\delta=\omega\cot(\omega t_c/2)$. The stream reach was considered to act as a linear reservoir with $k^{-1}=5$ h.

Fig. 2 displays the two solutions: one with the original, full boundary condition [Eq. (13)] and the other, with the simplified boundary condition

$$q(t)=\gamma[H(t)-h_c] \tag{17}$$

where $h_c=0$ was chosen for clarity. In the first case scenario, the parameter values were prescribed as $\gamma=1\ \mathrm{m\,h^{-1}}$ and $D=0.5\ \mathrm{m^2\,h^{-1}}$, while in the second case, D $(=100\ \mathrm{m^2\,h^{-1}})$ was chosen large enough that the $h(0,t)\approx h_c$ constant assumption could be met. The value of the γ parameter was systematically changed in the model to obtain an outflow from the reach close to the original one, and it became $0.4\ \mathrm{m\,h^{-1}}$. Note that the flux across the stream–aquifer interface is regulated only by this single parameter in the simplified boundary condition case. In this latter case now, all the water is lost to the aquifer because streamflow does not sink below the starting zero value, while in the complete boundary-condition case, water from the aquifer is flowing back to the stream after some time, as expected. What Fig. 2 was meant to illustrate for our streamflow forecasting purposes, using an existing structure of a state-space approach, is that by properly choosing the value of the γ parameter, the simplified boundary condition [Eq. (17)] in itself can result in a stream-reach outflow that approximates an outflow obtainable with the original and correct boundary condition in combination with the linearized Boussinesq equation.

Eq. (17) can be written as

$$q(t)=\gamma[H(t)-h_c]=c_\gamma[s(t)-s_0] \tag{18}$$

where $c_\gamma\ [\mathrm{T^{-1}}]=$constant; $s(t)\ [\mathrm{L^2}]=$water stored in the stream per unit length, considered proportional to streamstage; and $s_0=$constant reference value of storage. Inserting Eq. (18) into Eq. (15) results in

$$\frac{dS_j(t)}{dt}=Q(x_{j-1},t)-(k+g)S_j+C_0 \tag{19}$$

where $g\ [\mathrm{T^{-1}}]$ and $C_0\ [\mathrm{L^3\,T^{-1}}]$ are constant terms, namely, $g=2c_\gamma$ and $C_0=gS_0$. With Eq. (19) the state equation of the continuous KMN cascade can be obtained which now includes simplified stream–aquifer interactions.

State-Space Discretization of Kalinin–Milyukov–Nash Cascade with Stream–Aquifer Interactions

Applying Eq. (19) over a series of stream reaches, one obtains an extended form of the KMN cascade

$$\begin{bmatrix} \frac{dS_1(t)}{dt} \\ \frac{dS_2(t)}{dt} \\ \vdots \\ \frac{dS_n(t)}{dt} \end{bmatrix} = \begin{bmatrix} -(k+g) & 0 & \cdots & 0 \\ k & -(k+g) & \ddots & \vdots \\ & \ddots & \ddots & 0 \\ 0 & & k & -(k+g) \end{bmatrix} \begin{bmatrix} S_1(t) \\ S_2(t) \\ \vdots \\ S_n(t) \end{bmatrix} + \begin{bmatrix} u(t)+C_0 \\ C_0 \\ \vdots \\ C_0 \end{bmatrix} \tag{20}$$

that now accounts for flow from the stream to the aquifer whenever $gS_j > C_0$ and the opposite direction otherwise. In both cases the flux across the stream–aquifer boundary is directly proportional to the magnitude of this difference. Note that Eq. (20) now has a source term, C_0, which ensures that during a drought period, the stream collects groundwater; thus, a downstream section of the stream can have larger accumulated flow volumes over the drought period than the upper section, reflecting what generally happens in a groundwater-fed stream. Also, whenever $gS_j > C_0$, the stream has a sink expected to result in decreased peakflow values. The model has four parameters: k, n, g, and C_0. If the values of g and C_0 are chosen correctly, then over a suitably long period the stream must always gain water from the aquifer due to recharge to the groundwater.

During discretization the new state-transition matrix becomes

$$\underline{\underline{\Phi}}(\Delta t) = \begin{bmatrix} e^{-(k+g)\Delta t} & 0 & \cdots & 0 \\ k\Delta t e^{-(k+g)\Delta t} & e^{-(k+g)\Delta t} & \ddots & \vdots \\ \vdots & \vdots & \ddots & 0 \\ \frac{(k\Delta t)^{n-1}}{(n-1)!} e^{-(k+g)\Delta t} & \frac{(k\Delta t)^{n-2}}{(n-2)!} e^{-(k+g)\Delta t} & \cdots & e^{-(k+g)\Delta t} \end{bmatrix} \tag{21}$$

while the $\mathbf{\Gamma}_1$ and $\mathbf{\Gamma}_2$ vectors transform into

$$\mathbf{\Gamma}_1(\Delta t) = \begin{bmatrix} \frac{1}{(k+g)} \frac{\Gamma(1,(k+g)\Delta t)}{\Gamma(1)} \left[1 + \frac{e^{-(k+g)\Delta t}}{\Gamma(1,(k+g)\Delta t)} - \frac{1}{(k+g)\Delta t}\right] \\ \frac{k}{(k+g)^2} \frac{\Gamma(2,(k+g)\Delta t)}{\Gamma(2)} \left[1 + \frac{[(k+g)\Delta t]e^{-(k+g)\Delta t}}{\Gamma(2,(k+g)\Delta t)} - \frac{2}{(k+g)\Delta t}\right] \\ \vdots \\ \frac{k^{n-1}}{(k+g)^n} \frac{\Gamma(n,(k+g)\Delta t)}{\Gamma(n)} \left[1 + \frac{[(k+g)\Delta t]^{n-1}e^{-(k+g)\Delta t}}{\Gamma(n,(k+g)\Delta t)} - \frac{n}{(k+g)\Delta t}\right] \end{bmatrix} \tag{22}$$

and

$$\mathbf{\Gamma}_2(\Delta t) = \begin{bmatrix} \frac{1}{(k+g)} \frac{\Gamma(1,(k+g)\Delta t)}{\Gamma(1)} \left[\frac{e^{-(k+g)\Delta t}}{\Gamma(1,(k+g)\Delta t)} - \frac{1}{(k+g)\Delta t}\right] \\ \frac{k}{(k+g)^2} \frac{\Gamma(2,(k+g)\Delta t)}{\Gamma(2)} \left[\frac{[(k+g)\Delta t]e^{-(k+g)\Delta t}}{\Gamma(2,(k+g)\Delta t)} - \frac{2}{(k+g)\Delta t}\right] \\ \vdots \\ \frac{k^{n-1}}{(k+g)^n} \frac{\Gamma(n,(k+g)\Delta t)}{\Gamma(n)} \left[\frac{[(k+g)\Delta t]^{n-1}e^{-(k+g)\Delta t}}{\Gamma(n,(k+g)\Delta t)} - \frac{n}{(k+g)\Delta t}\right] \end{bmatrix} \tag{23}$$

so that the new state equation is

$$\mathbf{S}(t+\Delta t) = \underline{\underline{\Phi}}(\Delta t)\mathbf{S}(t) + \mathbf{\Gamma}_1(\Delta t)u(t+\Delta t) - \mathbf{\Gamma}_2(\Delta t)u(t) + \mathbf{\Omega} \tag{24}$$

where the ith component of the new $n \times 1$ vector term, $\mathbf{\Omega}$, is

$$\Omega_i = C_0 \sum_{j=1}^{i} \frac{k^{i-j}}{(k+g)^{i-j+1}} \frac{\Gamma(i-j+1,(k+g)\Delta t)}{\Gamma(i-j+1)} \tag{25}$$

See the Appendix for the steps involved with the derivation of the new state equation. By recursion in Eq. (24), the output of the extended discrete cascade at $t = m\Delta t$ can be calculated as

$$Q_{\text{out}}(m\Delta t) = \mathbf{HS}(m\Delta t) = \mathbf{H}\underline{\underline{\Phi}}^m(\Delta t)\mathbf{S}(0) + \sum_{i=0}^{m-1} \mathbf{H}\underline{\underline{\Phi}}^{m-1-i}(\Delta t) \times [\mathbf{\Gamma}_1(\Delta t)u[(i+1)\Delta t] - \mathbf{\Gamma}_2(\Delta t)u(i\Delta t) + \mathbf{\Omega}] \tag{26}$$

where the $\mathbf{H}$ vector is the same as previously. Note that if $g = 0$, the original cascade is recaptured.

Model Demonstration and Conclusions

The effect of including simplified stream–aquifer interactions in the state-space formulation of the DLCM of the NHFS of Hungary is demonstrated in Figs. 3 and 4.

In Fig. 3 the daily instantaneous streamflow values of the Danube, measured at 6 a.m. each day at Baja, about 200 km

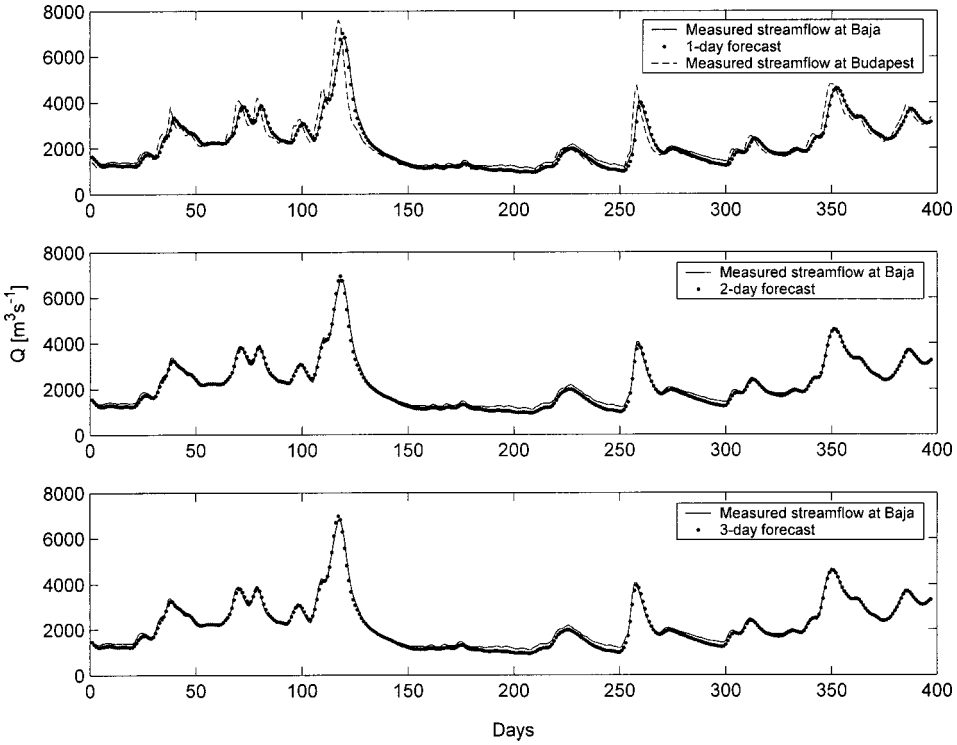

Fig. 3. Concurrent values of measured streamflow of Danube at 6 a.m. at Budapest and at Baja for April 13, 1991–May 17, 1992. 1–2–3-day forecasts of original model for Baja assumed perfect forecasts of similar lead times for Budapest. See Table 1 for model parameters and forecast statistics

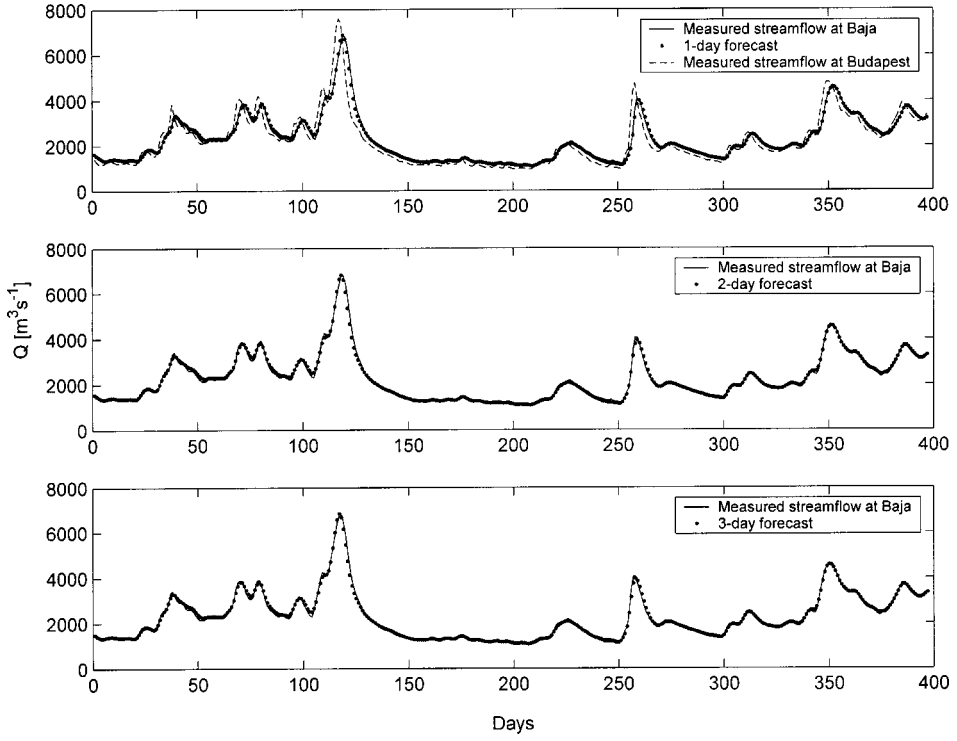

Fig. 4. Concurrent values of measured streamflow of Danube at 6 a.m. at Budapest and at Baja for April 13, 1991–May 17, 1992. The 1–2–3-day forecasts of extended model for Baja assumed perfect forecasts of similar lead times for Budapest. See Table 1 for model parameters and forecast statistics

Table 1. Optimized Parameter Values and Model Performance Statistics

Parameter	Original model	Extended model
n_{opt}	2	2
k_{opt} (day^{-1})	0.9	0.9
g_{opt} (day^{-1})	—	0.024
C_0 ($m^3\,s^{-1}$)	—	100.8
MRSE ($m^3\,s^{-1}$)	224.45	151.29
NSEC	98.36	99.26

$$(\%)=100\left[1-\frac{\Sigma(\hat{Q}_i-Q_i)^2}{\Sigma(Q_i-\overline{Q})^2}\right]$$

Note: Mean root-square error (MRSE), and Nash–Sutcliffe efficiency criterion (NSEC) for original and extended discrete cascades. Here $\overline{Q}=2{,}255\ m^3\,s^{-1}$ is mean streamflow (sample size=400) at Baja. Hat denotes forecasted streamflow values.

downstream of Budapest (with negligible tributary inflow to the reach), is forecasted by the original model using values at Budapest measured concurrently. For the 1 day forecast at Baja, measured values at Budapest on the previous and the forecasted day are used, and similarly, for the 2 day forecast, measured values at Budapest on the forecasted day plus the previous two days are used, and so on for the 3 day forecast. This simulates a ''perfect forecast'' scenario for Budapest which, however, is never the case, but by doing so, any systematic errors in the forecasts for the upstream station can be prevented from propagating to the downstream one. This practice of using forecasts for an upstream station to predict values at a downstream location is standard routine at hydrological services where the objective is to utilize every available bit of information that may improve forecasts for a given location. Depending on the accuracy of the forecasts for an upstream location, forecasting errors for a downstream location generally do improve. The two parameters of the discrete cascade, k and n, were optimized by trial and error when minimizing a mean root-square error (MRSE) term between forecasts and observations combined for all three leadtimes. This means that an MRSE term was calculated for each lead time over the period of observations and then their sum calculated. An optimal value of k and n were decided when this sum reached a minimum from systematically chosen trial values of k and n. An extra advantage of analytical solutions, in addition to that already mentioned, is that they can be recalculated very fast with different parameters, which is of importance in operative forecasting, especially when a large number of gaging stations are involved.

The same was performed with the extended cascade's four parameters. See Fig. 4 for improved model performance and Table I for the optimized values of the parameters and error statistics. As evident in Fig. 3, the original model undershoots the streamflow during low-flow periods, since there is no source term involved that would account for baseflow that becomes dominant during drought periods. The extended model, however, in Fig. 4 can account for this extra source of water supplied to the stream by the aquifer through its source term C_0. Similarly, the original model overshoots the largest, 15 year flood of Fig. 3, while the extended model (Fig. 4) accounts for bank storage during flood events and so provides a more accurate peakflow forecast. Note that the models were run without being updated each day through the error term.

The initial value of $\mathbf{S}(0)$ was calculated for each model using the inversion described by Szöllősi-Nagy (1987). By including simplified stream–aquifer interactions in the streamflow forecasting model, an improvement of 30% was achieved (Table 1) in the MRSE term for the chosen period of observations. The forecast improvement is also reflected in the Nash–Sutcliffe efficiency criterion (NSEC) value, which increased by about a percentage point (Table 1), which is significant when the NSEC value is already close to 100%.

In summary, a discrete state-space formulation of the continuous KMN cascade was introduced, currently used by the NHFS in Hungary for operational streamflow forecasting for the Danube and its tributaries. The discretization uses a sample-data system framework. The model was extended to account for simplified stream–aquifer interactions and the corresponding state equation was derived. Model performance was demonstrated on a 200 km reach of the Danube in Hungary with negligible tributary inflow. The extended model resulted in improved error statistics.

In operational use, the parameters of a forecasting model may be updated from time to time or even daily (Young 2002) to reflect short-term, seasonal, or longer-term changes in the watershed. Such investigations are outside the scope of the present study. For example, if the C_0 parameter turns out to display seasonal changes and if those changes are deemed significant enough to affect forecast accuracy in operational use, its value can also be updated, together with other parameter values, with the required frequency. Here the emphasis was on modifying an existing state-space structure of a hydrological model that is currently in operational use to allow for the inclusion of some simplified form of stream–aquifer interactions in the hope that doing so will eventually result in improved operational forecasts.

Acknowledgments

The writer is grateful to Charles Flowerday, Gabor Balint and two anonymous reviewers for their valuable comments on an earlier version of the manuscript.

Appendix

Derivation of the state-transition matrix $\underline{\underline{\Phi}}$ in Eq. (6) can be found in Szöllősi-Nagy (1982). The same steps were required for deriving $\underline{\underline{\Phi}}$ of the extended model in Eq. (24). For the derivation of the input-transition vectors, $\mathbf{\Gamma}_1$, $\mathbf{\Gamma}_2$, and $\mathbf{\Omega}$, one can start from the following equation (Szöllősi-Nagy 1982) representing a stream reach

$$\mathbf{S}(t+\Delta t)=\underline{\underline{\Phi}}(\Delta t)\mathbf{S}(t)+\int_t^{t+\Delta t}\underline{\underline{\Phi}}(t+\Delta t-\tau)\underline{\underline{G}}I(\tau)d\tau$$

$$=\underline{\underline{\Phi}}(\Delta t)\mathbf{S}(t)+\int_t^{t+\Delta t}\underline{\underline{\Phi}}(t+\Delta t-\tau)\times\underline{\underline{G}}[u(\tau)+C_0,C_0,\ldots,C_0]'d\tau \quad (27)$$

where the prime denotes the transpose, $\underline{\underline{G}}=n\times n$ input-distribution matrix, which now becomes an identity matrix due to a vector input $\mathbf{I}(t)$, and where it will now be assumed that the upstream flow value $u(t)$ changes linearly between measured values at t and $t+\Delta t$. Note that Szöllősi-Nagy (1982) gave the derivation for a scalar-valued input $u(t)$, which is constant in the interval $[t,t+\Delta t)$ that is closed from the left and open from the right.

For sake of clarity, the steps will be demonstrated on the ith element of the vectors involved. The ith element of Eq. (27), provided the system is relaxed at time t [i.e., $\mathbf{S}(t)=0$], can be written as

$$S_i(t+\Delta t)=\int_t^{t+\Delta t}\left[\Phi_{i,1}(t+\Delta t-\tau)u(\tau)+C_0\sum_{j=1}^{i}\Phi_{i,j}(t+\Delta t-\tau)\right]d\tau \quad (28)$$

where the lower-triangular property of $\underline{\underline{\Phi}}$ was utilized.

The first term on the right-hand side (r.h.s) of Eq. (28) can be written as

$$\begin{aligned}&\int_t^{t+\Delta t}\Phi_{i,1}(t+\Delta t-\tau)u(\tau)d\tau\\&=\int_t^{t+\Delta t}\Phi_{i,1}(t+\Delta t-\tau)\left[u(t)+\frac{u(t+\Delta t)-u(t)}{\Delta t}(\tau-t)\right]d\tau\\&=\int_t^{t+\Delta t}\left[\Phi_{i,1}(t+\Delta t-\tau)u(t)+\Phi_{i,1}(t+\Delta t-\tau)\times\frac{u(t+\Delta t)-u(t)}{\Delta t}\tau-\Phi_{i,1}(t+\Delta t-\tau)\times\frac{u(t+\Delta t)-u(t)}{\Delta t}t\right]d\tau\end{aligned} \quad (29)$$

where the sample-data system framework was used to obtain the $u(\tau)$ values between two discrete measurements. Performing a change of variables, $\tau^*=t+\Delta t-\tau$, the first term on the r.h.s. of the integral transforms into

$$\begin{aligned}&u(t)\frac{k^{i-1}}{(i-1)!}\int_0^{\Delta t}\frac{\tau^{*(i-1)}}{e^{c^*\tau^*}}d\tau^*\\&=u(t)\frac{k^{i-1}}{(k+g)^i}\frac{1}{(i-1)!}\Gamma(i,(k+g)\Delta t)\\&=u(t)\frac{k^{i-1}}{(k+g)^i}\frac{\Gamma(i,(k+g)\Delta t)}{\Gamma(i)}\end{aligned} \quad (30)$$

where $\Phi_{i,1}$ from Eq. (21), and $c^*=(k+g)$ were used. Similarly, the third term of Eq. (29) will yield

$$\frac{k^{i-1}}{(k+g)^i}\frac{t[u(t)-u(t+\Delta t)]}{\Delta t}\frac{\Gamma(i,(k+g)\Delta t)}{\Gamma(i)} \quad (31)$$

whereas the second term becomes

$$\begin{aligned}&\frac{k^{i-1}}{(i-1)!}\frac{u(t+\Delta t)-u(t)}{\Delta t}\int_0^{\Delta t}\frac{\tau^{*(i-1)}}{e^{c^*\tau^*}}(t+\Delta t-\tau^*)d\tau^*\\&=\frac{k^{i-1}}{(i-1)!}\frac{u(t+\Delta t)-u(t)}{\Delta t}\left[\frac{t+\Delta t}{(k+g)^i}\Gamma(i,(k+g)\Delta t)-\int_0^{\Delta t}\frac{\tau^{*i}}{e^{c^*\tau^*}}d\tau^*\right]\\&=\frac{k^{i-1}}{(i-1)!}\frac{u(t+\Delta t)-u(t)}{\Delta t}\frac{1}{(k+g)^i}\left[(t+\Delta t)\Gamma(i,(k+g)\Delta t)-\frac{1}{k+g}\Gamma(i+1,(k+g)\Delta t)\right]\\&=\frac{k^{i-1}}{(k+g)^i}\frac{u(t+\Delta t)-u(t)}{\Delta t}\frac{1}{\Gamma(i)}\left[(t+\Delta t)\Gamma(i,(k+g)\Delta t)-\frac{i\Gamma(i,(k+g)\Delta t)}{k+g}+[(k+g)\Delta t]^ie^{-(k+g)\Delta t}\right]\end{aligned} \quad (32)$$

where the algebraic identities $\Gamma(i+1,x)=i\Gamma(i,x)-x^ie^{-x}$ and $\Gamma(i)c^{-i}=\int_0^\infty x^{i-1}e^{-cx}dx$ were used (Abramowitz and Stegun 1965).

After combining all three terms, one obtains

$$\begin{aligned}&\int_t^{t+\Delta t}\Phi_{i,1}(t+\Delta t-\tau)u(\tau)d\tau\\&=\frac{k^{i-1}}{(k+g)^i}\frac{\Gamma(i,(k+g)\Delta t)}{\Gamma(i)}\times[[1+\Lambda_i(\Delta t)]u(t+\Delta t)-\Lambda_i(\Delta t)u(t)]\end{aligned} \quad (33)$$

with Λ_i being

$$\Lambda_i(\Delta t)=\frac{[(k+g)\Delta t]^{i-1}e^{-(k+g)\Delta t}}{\Gamma(i,(k+g)\Delta t)}-\frac{i}{(k+g)\Delta t} \quad (34)$$

When $j=1$ in the second term of the r.h.s. of Eq. (28) one obtains Eq. (30) with C_0 replacing $u(t)$, the latter being just a constant, since t is set now. By keeping track of the value of j in Eq. (28) behind the summation sign, one obtains Eq. (25). The ith line of $\mathbf{\Gamma}_1$, $\Gamma_1^{(i)}$ is simply defined as

$$\Gamma_1^{(i)}(\Delta t)=\frac{k^{i-1}}{(k+g)^i}\frac{\Gamma(i,(k+g)\Delta t)}{\Gamma(i)}[1+\Lambda_i(\Delta t)] \quad (35)$$

and similarly, $\Gamma_2^{(i)}$ as

$$\Gamma_2^{(i)}(\Delta t)=\frac{k^{i-1}}{(k+g)^i}\frac{\Gamma(i,(k+g)\Delta t)}{\Gamma(i)}\Lambda_i(\Delta t) \quad (36)$$

References

Abramowitz, M., and Stegun, I. A. (1965). *Handbook of mathematical functions*, Dover, New York.

Chow, V. T., Maidment, D. R., and Mays, L. W. (1988). *Applied hydrology*, McGraw-Hill, New York.

Cunge, J. A. (1969). "On the subject of a flood propagation model (Muskingum method)." *J. Hydraul. Res.*, 7, 205–230.

Hantush, M. M., Harada, M., and Marino, M. A. (2001). ''Hydraulic analysis of baseflow and bank storage in alluvial streams.'' *Proc., Wetlands Eng. River Restor.*, Reno, Nev.

Hantush, M. M., Harada, M., and Marino, M. A. (2002). ''Hydraulics of stream flow routing with bank storage.'' *J. Hydrologic Eng.*, 7(1), 76–89.

Hunt, B. (1990). ''An approximation for the bank storage effect.'' *Water Resour. Res.*, 26(11), 2769–2775.

Kalinin, G. P., and Milyukov, P. I. (1957). ''Raschete neustanovivshegosya dvizheniya vody v otkrytykh ruslakh (On the computation of unsteady flow in open channels).'' *Met. Gydrologia Zhurnal*, 10, 10–18.

Kalman, R. E. (1960). ''A new approach to linear filtering and prediction problems.'' *ASME J. Basic Eng.*, 82D, 35–45.

Kalman, R. E., and Bucy, R. S. (1961). ''New results in linear filtering and prediction theory.'' *J. Basic Eng.*, 83, 95–103.

Moench, A. F., Sauer, V. B., and Jennings, M. E. (1974). ''Modification of routed streamflow by channel loss and baseflow.'' *Water Resour. Res.*, 10(5), 963–968.

Nash, J. E. (1957). ''The form of instantaneous unit hydrograph.'' *Proc., IASH Assemblee Generrale de Toronto*, Toronto, 114–131.

Pearce, F. (2002). ''Europe's wake-up call.'' *New Sci.*, August 24, 1.

Pinder, G. F., and Sauer, S. P. (1971). ''Numerical simulation of flood wave modification due to bank storage effects.'' *Water Resour. Res.*, 7(1), 63–70.

Szilagyi, J. (2003). ''State-space discretization of the KMN-cascade in a sample-data system framework for streamflow forecasting.'' *J. Hydrologic Eng.*, 8(6), 339–347.

Szilagyi, J., Harvey, F. E., and Ayers, J. F. (2003). ''Regional estimation of base recharge to ground water using water balance and a base-flow index.'' *Ground Water*, 41(4), 504–513.

Szöllősi-Nagy, A. (1982). ''The discretization of the continuous linear cascade by means of state space analysis.'' *J. Hydrol.*, 58, 223–236.

Szöllősi-Nagy, A. (1987). ''Input detection by the discrete linear cascade model.'' *J. Hydrol.* 89, 353–370.

Szöllősi-Nagy, A. (1989). A mederbeli lefolyás real-time előrejelzése dinamikus strukturális-sztochasztikus modellekkel (real-time streamflow forecasting using dynamically structured deterministic-stochastic models), Vizgazdálkodási Tudományos Kutató Központ, Budapest, Hungary.

Young, P. C. (2002). ''Advances in real-time flood forecasting.'' *Philos. Trans. R. Soc. London, Ser. A*, 360, 1433–1450.

Zitta, V. L., and Wiggert, J. M. (1971). ''Flood routing in channels with bank storage.'' *Water Resour. Res.*, 7(5), 1341–1345.